Molecular description of constant-load stretching of amorphous poly(ethylene terephthalate) films

G. Lorentz
Rhône-Poulenc Films, Magphane International, Saint Maurice de Beynost, BP 140, 01701 Miribel Cedex, France

and J. F. Tassin*
Laboratoire de PhysicoChimie Macromoléculaire, URA CNRS no. 509, Université du Maine, Avenue Olivier Messiaen, 72017 Le Mans Cedex, France
(Received 30 December 1993)

This paper is devoted to a molecular description of the deformation of amorphous isotropic poly(ethylene terephthalate) (PET) films at temperatures slightly above the glass transition temperature under constant load. The deformation is qualitatively described by chain relaxation phenomena occurring before stress-induced crystallization, which are followed by the equilibration of a rubber-like network. The junction points include both trapped entanglements and crystalline units. The structure of this network is characterized by the number of segments between crosslinks. This parameter is calculated by comparing the predictions of the rubber elasticity theory (without Gaussian approximation) with the experimentally observed draw ratios under given conditions of temperatures and loads. It is shown that light loads induce soft networks leading to high draw ratios. The predictions of the molecular orientation derived from this treatment are in good agreement with birefringence data on a large variety of samples.

(Keywords: PET films; orientation; relaxation)

INTRODUCTION

In the conventional flat-film processing of poly(ethylene terephthalate) (PET), the molten film extruded from a flat die is first quenched on a cold roll, leading to an amorphous supercooled melt. It is then stretched at temperatures close to the glass transition temperature, T_g, under a constant drawing force between rolls having differential tangential speeds. Subsequent steps involve a transverse stretching followed by thermosetting treatment at high temperatures. In order to accurately study the longitudinal stretching process, a laboratory-scale set-up, able to reproduce constant-load stretching under well-defined experimental conditions, has been designed[1,2]. The kinetics of deformation, and the structure and orientation properties of the films have been detailed previously[1-6].

The aim of this paper is to analyse the mechanical response and the optical anisotropy of the material using a molecular deformation model. This paper is divided into four parts. In the first part, the basic features of the deformation process are recalled and a qualitative interpretation is proposed. The second part is devoted to the mechanical analysis of the deformation process using the classic rubber-like elasticity of a trapped network. In the third part, the build-up of the trapped network and its resulting structure are interpreted in the context of the Doi–Edwards model. Finally, the model predictions are compared with experimental data.

DESCRIPTION OF THE DEFORMATION PROCESS

As amorphous PET film is subjected to drawing under constant engineering stress, at temperatures slightly above T_g, the deformation is characterized by the following features, which are outlined in *Figure 1*[1,2].

(1) The deformation starts slowly and the rate of deformation, defined as $\dot{\varepsilon}=(1/L_s)(dL_s/dt)$ (where L_s is the length of the sample), increases with time until it reaches a maximum. The deformation kinetics then slow down and the draw ratio reaches a constant value (plateau draw ratio, λ_p).

(2) The kinetics of deformation increase with the applied stress and the stretching temperature. For example, for an engineering stress of 4 MPa and for conventional PET ($M_w=40\,000\,g\,mol^{-1}$), the maximum rate of deformation is on the order of $0.1\,s^{-1}$ at 80°C and $20\,s^{-1}$ at 97°C. Under these conditions, typical stretching times to reach the plateau draw ratio are 15 s at 80°C and 0.3 s at 97°C. For an engineering stress of 2 MPa, the maximum rate is around $10^{-2}\,s^{-1}$ at 80°C and $5\,s^{-1}$ at 97°C.

The variation of the plateau draw ratio with temperature and load, depicted in *Figure 2*, is more complex. At any

* To whom correspondence should be addressed

0032-3861/94/15/3200–06

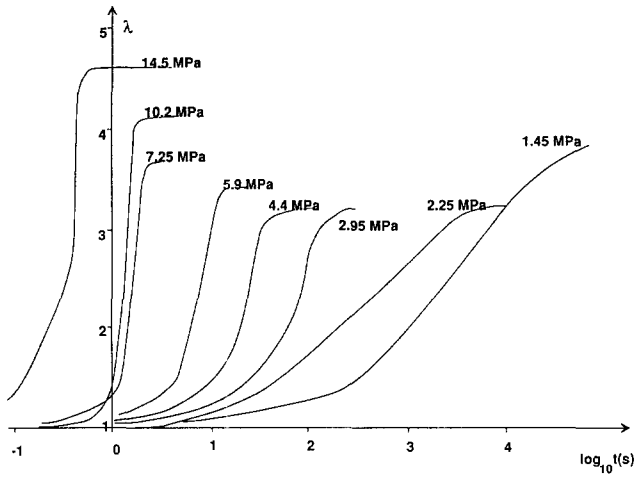

Figure 1 Draw ratio *versus* time during constant-load stretching at 80°C with various engineering stresses. (Data from references 1 and 2)

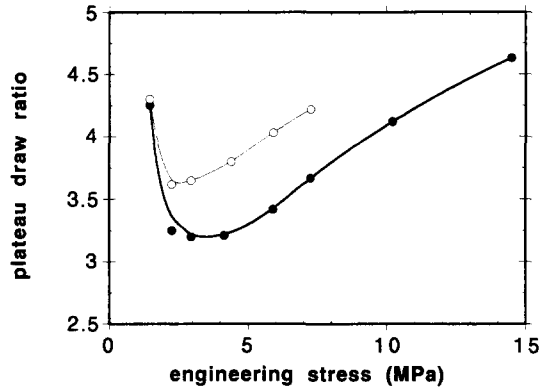

Figure 2 Plateau draw ratio *versus* applied engineering stress at 80°C (●) and 97°C (○). (Data from references 1 and 2)

temperature a minimum plateau draw ratio is observed for an applied stress of 2.5 MPa. For stresses higher than 2.5 MPa the plateau draw ratio increases, whereas for lower stresses the plateau draw ratio increases if the stress decreases. At very low stresses (0.6 MPa), large values of the plateau draw ratio (such as $\lambda_p = 9$) can be obtained, even at low temperatures (80°C).

The fact that the rate of deformation goes through a maximum has been attributed to the onset of crystallization induced by the molecular orientation. Owing to crystallization, a physical network builds up in the material, the crystallites preventing long-range motion of the chains. This network reaches an equilibrium deformation under the applied load, as shown by the existence of a plateau draw ratio. According to the classic description of rubber-like elasticity[7], the larger the applied stress, the higher the equilibrium deformation at a given network density. Large draw ratios under low stresses must be connected to low network densities. Therefore, the existence of two regimes in the stress dependence of the equilibrium draw ratio can be understood as follows. At large stresses, the expected load dependence is observed, indicating a rather constant network density. On the other hand, at low stresses the network density must be lower, so that larger extensions are reached. In order to quantitatively check this behaviour, the molecular network has to be characterized under our experimental conditions. This goal will be achieved by comparing the experimental relationships between applied loads and equilibrium draw ratios with the predictions of the theory of rubber-like elasticity.

QUANTITATIVE CHARACTERIZATION OF THE PHYSICAL NETWORK

In order to calculate the number of links between junction points at equilibrium deformation under the applied load, the classic rubber-like elasticity theory has been used without the Gaussian approximation[7]. The nature of junction points (crystallites or trapped entanglements) does not play any role in our calculations, provided that the crystalline entities remain small with respect to the chain dimensions and that the change of the density induced by the crystalline phase is negligible, which limits our approach to low crystallinity samples. The error introduced by this assumption is small and is discussed in Appendix 1.

We basically assume that the true stress at equilibrium is equal to the entropic stress arising from the deformation of the subchains between junction points. The plateau draw ratio, λ_p, is related to the true stress, σ_v, by the following expression (derived in Appendix 2, equation (A5)):

$$\sigma_v = \frac{\rho RT}{3M_s} \lambda_{max} \lambda_p L^{-1}\left(\frac{\lambda_p}{\lambda_{max}}\right) \quad (1)$$

where ρ is the polymer mass per unit volume (1.336×10^3 kg m^{-3}), R is the gas constant, T is the absolute temperature, M_s is the average molecular mass per subchain, λ_{max} is the maximum draw ratio for such a subchain, and L^{-1} is the inverse Langevin function. Expression (1) contains two unknown but interrelated quantities, M_s and λ_{max}. The relationship between them (derived in Appendix 3, expression (A8)) is based on the conformational properties of the PET repeat unit[8]. Therefore, if σ_v, λ_p and the stretching temperature are experimentally obtained, M_s or λ_{max} can be computed.

FORMATION OF A TRAPPED NETWORK

As far as rheological properties of polymer melts are concerned, these materials are often described in terms of a non-permanent network of entanglements, on the basis of the elastic plateau observed in dynamic mechanical experiments. The plateau modulus of PET has been determined as $G_N^0 = 3.1$ MPa at 548 K, leading to an average molecular weight between entanglements[9] of $M_e = 1450$ g mol^{-1}, in agreement with another determination[10] made directly on the PET used in this study, which yields $M_e = 1200$ g mol^{-1}.

In order to evaluate the potential elasticity of this entanglement network, we use the conformational results of Flory[8] (Appendix 3) and calculate the maximum draw ratio λ_{max}. Let us call r the projection along the drawing axis of the end-to-end vector of a subchain between entanglements in the isotropic state. λ_{max} can be defined as:

$$\lambda_{max} = \frac{L}{r} \quad (2)$$

where L is the total contour length of the subchain. Using the results of Appendix 3, we deduce a maximum draw

ratio of $\lambda_{max}=3.45$, defining the limiting elasticity of the entanglement network assumed to act as a fixed network without any slipping of entanglement points. Experimental data, obtained on samples drawn with light loads in the laboratory experiment, show that much higher deformations can be reached. They can be explained by relaxation processes occurring at the beginning of the stretching process.

In order to give a molecular description of these relaxation processes, we base our discussion on the Doi–Edwards model[11], which describes the relaxation of a melt suddenly subjected to a step strain. In the model, any chain is confined inside a tube resulting from the constraints exerted by the surrounding chains. After stretching, the tube is affinely deformed and relaxation of the chain towards the random coil isotropic conformation occurs. The relaxation is achieved in three steps, well separated in time. At short times, a Rouse relaxation of part of the chain between entanglements is observed. This process, essentially local, is characterized by a relaxation time, τ_A, independent of the molecular weight of the chain. The second process is a retraction of the deformed chain inside its deformed tube in order to recover the equilibrium curvilinear monomer density. It is worth noting that this retraction process involves an increase of the average number of monomers between entanglements. The relaxation time, τ_B, scales as the square of the molecular weight of the chain. Finally, isotropic orientation of chain segments is achieved by a reptation motion. The time, τ_C, associated with this process scales as the third power of the molecular weight.

The step strain experiment, on which the theoretical description of the relaxation is based, is completely different from our deformation history. In order to understand how relaxation processes occur in our experiments, we refer to *Figure 1*, which shows that the deformation experiences very low strain rates, especially at the beginning of the stretching process before the onset of crystallization. If we define $\dot{\varepsilon}$ as the instantaneous strain rate, a relaxation process with a relaxation time τ will be effective if $\dot{\varepsilon}\tau$ is on the order of 1 (Deborah number criterion). For $\dot{\varepsilon}\tau \ll 1$, the relaxation process has sufficient time to occur, whereas it is frozen if $\dot{\varepsilon}\tau \gg 1$. Our experiment, in contrast to constant-strain-rate tests often used in conventional rheometry, sweeps over a large domain of strain rates, so that different relaxation processes can be efficient during the deformation.

The very first stages of the deformation involve the reptation of the chains as long as $\dot{\varepsilon}\tau_C < 1$. In practice, at temperatures close to T_g, the reptation times are very long (on the order of 10^4 s at 80°C (ref. 10)), so that this process only occurs at the very beginning of the stretching, where the increase of sample length is negligible. The average distance between entanglements remains constant during this process so that the entanglement network is unchanged.

At longer times, retraction processes may occur and their efficiency is enhanced by an increasing deformation. The retraction process leads to an increase of the molecular weight between entanglements. As $\dot{\varepsilon}$ increases, the large-scale retraction process becomes too slow to be efficient and the trapped subchains orientate strongly. When the orientation of the chain axes becomes higher than a critical value, induced crystallization appears[12], thereby trapping any large-scale motion of the chains. Finally, subchains trapped by crystallites will continue to deform (and eventually to crystallize) until their entropic reaction equals the applied stress.

This qualitative description is valid whatever the applied load, the stretching temperature and the molecular weight of the polymer. It is now relatively straightforward to understand the variation of the plateau draw ratio with the applied load. As noted previously, small stresses lead to relatively low strain rates. Therefore, retraction motions may occur during a longer time, creating a looser network. For larger loads, the trapped network does not depend strongly on the applied stress since the time allowed for the retraction process becomes smaller and smaller. Moreover, retraction appears restricted to small deformations and is therefore less efficient in modifying the network.

COMPARISON WITH EXPERIMENTS

Model validation by birefringence data

In order to check this approach we use the measured birefringence in the film plane of stretched samples, from which the second moment of the orientation distribution function of the chain axes relative to the draw direction can be derived[13]. The second moment of the orientation distribution function is defined as:

$$P_2 = \tfrac{1}{2}\langle 3\cos^2\theta - 1\rangle \tag{3}$$

where θ is the angle between the chain axis and the draw direction and the angle brackets denote an average over all the elementary units. If the polymer chains are able to crystallize, information on the orientation averaged over the amorphous and the crystalline phases is obtained.

For the purpose of a P_2 calculation, the real distribution of orientation can be replaced by a fraction, P_2, of chains fully aligned along the draw direction and a fraction, $(1-P_2)$, of chains isotropically distributed[14]. Although the deformation is uniaxial planar, we use the above decomposition, which assumes uniaxial symmetry, since the calculation of stress validates the uniaxial approximation, as checked in Appendix 2, as well as previous extensive measurements on samples drawn under similar conditions[3–6].

Since P_2 represents the fraction of fully oriented segments, it is expected that $P_2=1$ for the fully oriented polymer drawn at λ_{max}, and $P_2=0$ for the initial undrawn isotropic film. We assume, as a first approximation, that P_2 is proportional to the fraction of chains drawn at λ_{max} inside the sample, or equivalently that:

$$P_2 = \frac{\lambda_p - 1}{\lambda_{max} - 1} \tag{4}$$

in order to account for this proportionality and limiting conditions given above. This equation exhibits a relationship between the molecular orientation and the structure of the network which determines λ_{max}.

Since highly oriented segments will tend to crystallize during deformation, the contribution of the crystalline phase has to be taken into account and we expect the orientation calculated by expression (4) to reflect the average orientation inside the material. P_2 can thus be calculated from a knowledge of λ_{max} and compared with birefringence data. In order to evaluate λ_{max}, we apply the rubber-like elasticity theory (equation (1)) using the experimental values of true stress and plateau draw ratio.

The relationship between the calculated P_2 and the birefringence Δn of 22 samples, stretched under different stress and temperature conditions, is plotted in *Figure 3*. The birefringence Δn is calculated from the refractive indices along the principal directions of the film by:

$$\Delta n = n_1 - \frac{n_2 + n_3}{2} \quad (5)$$

where subscript 1 is the draw direction, subscript 2 is the direction perpendicular to the plane of the film and subscript 3 is in the plane of the film, perpendicular to the draw direction. (The refractive indices were measured using an Abbe refractometer.) A linear relationship between P_2 and the birefringence is observed. The slope, obtained from a least-squares regression, yields $\Delta n = 0.24 P_2$. The proportionality factor between birefringence and orientation (0.24) is close to the intrinsic birefringence of PET[15-17] ($\Delta n^\circ = 0.22$) expected under uniaxial symmetry. This agreement acts in favour of our model, despite the approximations involved in its derivation.

Evolution of the network structure

The evolution of the network characteristics as a function of applied stress and temperature is plotted in *Figure 4*. The mesh size of the network decreases with the applied stress, especially for stresses below 2.5 MPa. The influence of temperature is weaker but an increase in temperature still induces a softer network. It is

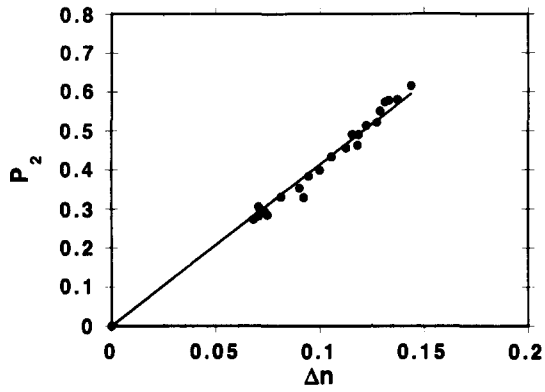

Figure 3 Calculated P_2 *versus* in-plane birefringence for 22 PET samples (various molecular weights, temperatures and stresses). The slope of the line is 4.138

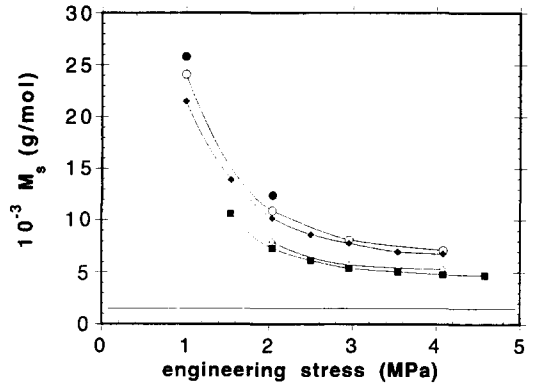

Figure 4 Calculated network mesh size M_s *versus* engineering stress for a PET with $M_w = 40\,000\ g\ mol^{-1}$ for various stretching temperatures: ■, 90°C; ◇, 95°C; ◆, 100°C; ○, 105°C; ●, 110°C. (The horizontal line is relative to the molecular weight between entanglements in amorphous PET)

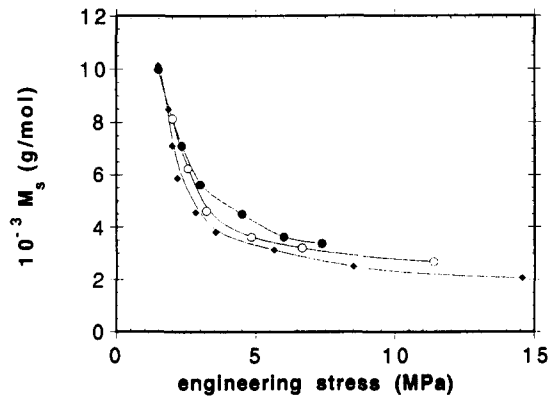

Figure 5 Calculated network mesh size M_s *versus* engineering stress at a stretching temperature of 95°C for PET of various molecular weights (M_w in g mol^{-1}): ◆, 80 000; ○, 40 000; ●, 30 000

interesting to note that at a given stress a relatively large difference in the networks is observed between stretching temperatures of 95 and 100°C. The existence of such behaviour has already been observed using spectroscopic techniques to characterize the molecular orientation of drawn samples[4,5,18]. The present mechanical analysis is fully consistent with these previous observations.

The influence of the molecular weight of the PET chains is depicted in *Figure 5*. For a given stress, the highest molecular weight PET shows the highest network density. This behaviour is easily explained by the fact that higher molecular weights imply longer relaxation times and thus less relaxation during the stretching process. The mesh size of the induced network is therefore smaller. It appears that even at the highest stresses and highest molecular weights, the mesh size is slightly higher than the molecular weight between entanglements.

From *Figures 4* and *5* we may conclude that the structure of the network is highly dependent on relaxation phenomena occurring at the early stages of the creep experiment, in agreement with the model depicted above.

CONCLUSIONS

Although involving rather crude approximations, a model based on the rubber-like elasticity theory with a variable number of links between junction points has been able to account for the mechanical behaviour of amorphous PET films deformed under constant load at temperatures slightly above the glass transition temperature.

The very large deformation ratios (much larger than the maximum draw ratio of the entanglement network) obtainable under light loadings have been explained on the basis of relaxation processes occurring at the early stages of stretching, prior to the onset of stress-induced crystallization. Following the Doi–Edwards description of polymer dynamics, it is possible to identify this relaxation process mainly as the retraction of the chains inside their tubes. This description of the deformation of amorphous PET as a molecular network is in agreement with spectroscopic data obtained on samples drawn under similar conditions[5,18].

In the final state of the film, the stress-induced crystallization leads to the connection of all the chains in a macroscopic network. The equilibrium deformation is related to the number of 'junctions' per unit volume.

These 'junctions' consist of crystalline blocks formed during stretching as well as entanglements trapped between crystalline structures.

REFERENCES

1 Le Bourvellec, G., Beautemps, J. and Jarry, J. P. *J. Appl. Polym. Sci.* 1990, **39**, 319
2 Le Bourvellec, G. and Beautemps, J. *J. Appl. Polym. Sci.* 1990, **39**, 329
3 Lapersonne, P., Tassin, J. F., Monnerie, L. and Beautemps, J. *Polymer* 1991, **32**, 3331
4 Lapersonne, P., Bower, D. I. and Ward, I. M. *Polymer* 1992, **33**, 1266
5 Lapersonne, P., Bower, D. I. and Ward, I. M. *Polymer* 1992, **33**, 1277
6 Lapersonne, P., Tassin, J. F. and Monnerie, L. *Polymer* 1994, **35**, 2192
7 Treloar, L. R. G. 'The Physics of Rubber Elasticity', 3rd edn, Clarendon Press, Oxford, 1975
8 Flory, P. J. 'Statistical Mechanics of Chain Molecules', Wiley-Interscience, New York, 1969
9 Wu, S. *J. Polym. Sci., Polym. Phys. Edn* 1989, **27**, 723
10 Le Bourvellec, G. Thesis Doct. Ing., Université Paris VI, 1984
11 Doi, M. and Edwards, S. F. 'The Theory of Polymer Dynamics', Clarendon Press, Oxford, 1986
12 Le Bourvellec, G., Jarry, J. P. and Monnerie, L. *Polymer* 1986, **27**, 856
13 Ward, I. M. *Adv. Polym. Sci.* 1985, **66**, 81
14 Irvine, P. A. and Smith, P. *Macromolecules* 1986, **19**, 240
15 Pinnock, P. R. and Ward, I. M. *Br. J. Appl. Phys.* 1964, **15**, 1559
16 Ward, I. M. *Proc. Phys. Soc.* 1962, **80** (5), 1176
17 Gupta, V. B. and Ramesh, C. *Polym. Commun.* 1987, **28**, 43
18 Lapersonne, P. Thesis de Doctorat de l'Université Paris VI, 1991
19 Daubeny, R., Bunn, C. W. and Brown, C. J. *Proc. R. Soc. London* 1954, **226**, 531

APPENDIX 1

Influence of the induced crystallinity

In our modelling of the PET film, even in the deformed state, we neglect the volume fraction of the crystalline phase and assume that the density is equal to the density of amorphous PET ($\rho_{am} = 1.336 \times 10^3$ kg m^{-3}). The error induced by this approximation is given, assuming a two-phase model by:

$$\frac{\rho - \rho_{am}}{\rho_{am}} = \frac{\chi(\rho_{cryst} - \rho_{am})}{\rho_{am}} < 0.1\chi$$

taking $\rho_{cryst} = 1.457 \times 10^3$ kg m^{-3}. For crystalline volume fractions lower than 30% (which is the case for our samples[3]), the relative error is less than 3%. Furthermore, the eventual densification of the amorphous phase leads to a reduced mismatch.

The morphology of the crystalline structure produced in this type of stretching has been analysed previously[3]. The structure consists of rather small crystalline blocks with chain axes highly oriented along the draw direction. The size of the crystalline blocks is around 2.5 nm × 3 nm × 5 nm along the film normal direction, the width and the stretching direction, respectively. Comparing these dimensions of the unit cell ($4.5 \times 5.9 \times 10.7$ Å^3), it appears that relatively few unit cells are gathered in these blocks (roughly five along each direction).

APPENDIX 2

Derivation of the expression of the stress

Following Treloar[7], the difference of principal stresses, σ_i, in a pure homogeneous strain of the most general type is given by:

$$\sigma_1 - \sigma_2 = \frac{\rho RT}{3M_s}\frac{L}{r}\left[\lambda_1 \boldsymbol{L}^{-1}\left(\frac{\lambda_1 r}{L}\right) - \lambda_2 \boldsymbol{L}^{-1}\left(\frac{\lambda_2 r}{L}\right)\right] \quad \text{(A1)}$$

where ρ is the polymer mass per unit volume, M_s is the molar mass of the elastic subchain, R is the gas constant, and T is the absolute temperature; r is the projection along one of the principal axes of the end-to-end distance of a subchain in the isotropic state, L is the subchain contour length, λ_i is the extension ratio along principal axis i, and $\boldsymbol{L}^{-1}$ is the inverse Langevin function.

At the maximum extension ratio, the chain is totally extended:

$$\lambda_{max} r = L \quad \text{(A2)}$$

Equation (A1) can thus be rewritten as:

$$\sigma_1 - \sigma_2 = \frac{\rho RT}{3M_s}\lambda_{max}\left[\lambda_1 \boldsymbol{L}^{-1}\left(\frac{\lambda_1}{\lambda_{max}}\right) - \lambda_2 \boldsymbol{L}^{-1}\left(\frac{\lambda_2}{\lambda_{max}}\right)\right] \quad \text{(A3)}$$

Under uniaxial-planar conditions, if subscript 1 is the draw direction and subscript 2 is the direction normal to the film plane, then $\lambda_1 = \lambda$ and $\lambda_2 = 1/\lambda$, where λ is the extension ratio.

No stress, except the hydrostatic pressure, is acting along direction 2, so that the stretching stress can be expressed as:

$$\sigma = \frac{\rho RT}{3M_s}\lambda_{max}\left[\lambda \boldsymbol{L}^{-1}\left(\frac{\lambda}{\lambda_{max}}\right) - \frac{1}{\lambda}\boldsymbol{L}^{-1}\left(\frac{1}{\lambda\lambda_{max}}\right)\right] \quad \text{(A4)}$$

For draw ratios $\lambda > 3$, the second term in equation (A4) is almost negligible so that the expression of σ can be simplified as:

$$\sigma = \frac{\rho RT}{3M_s}\lambda_{max}\lambda \boldsymbol{L}^{-1}\left(\frac{\lambda}{\lambda_{max}}\right) \quad \text{(A5)}$$

This expression of the stress is the same in the uniaxial case. The relative error induced by this simplification is less than 5.5% for $\lambda > 3$.

APPENDIX 3

Derivation of λ_{max} from conformational properties of PET

According to Flory[8], the PET repeat unit contains six flexible units, the average length of which is $l = 2.68$ Å for an average molecular weight of μ = monomer mass/6 = 32 g mol^{-1}.

Following the determination of Daubeny *et al.*[19], the projected length of the repeat unit in *trans* conformation along the chain axis is 10.75 Å, so that the average projected length per flexible unit is $l_p = 1.79$ Å. The number of flexible units between entanglements is:

$$N_e = M_e/\mu = 37.5$$

so that the extended length between entanglements is:

$$L = 1.79 N_e$$

If we assume the PET subchains to follow Gaussian statistics, the average end-to-end distance between entanglements is:

$$d = (N_e C_\infty l^2)^{1/2} \quad \text{(A6)}$$

and d is related to r, the projection of the end-to-end vector along one of the principal axes of the sample, by

$d^2 = 3r^2$. For PET, C_∞, the polymer characteristic ratio, has been calculated[9] as 4.2.

As the maximum draw ratio is defined as $\lambda_{max} = L/r$, one gets for λ_{max} the following expression:

$$\lambda_{max} = \frac{l_p}{l}\left(\frac{3N_e}{C_\infty}\right)^{1/2} \tag{A7}$$

which relates λ_{max} and N_e, since the other quantities are known. In the isotropic state, the calculation yields $\lambda_{max} = 3.45$. Equation (A7) can be generalized to relate the maximum draw ratio to the average number of links between junction points N_s as:

$$\lambda_{max} = \frac{l_p}{l}\left(\frac{3N_s}{C_\infty}\right)^{1/2} \tag{A8}$$